

## Research article

# THE EFFECTS OF RACKET INERTIA TENSOR ON ELBOW LOADINGS AND RACKET BEHAVIOR FOR CENTRAL AND ECCENTRIC IMPACTS

Steven M. Nesbit , Michael Elzinga, Catherine Herchenroder and Monika Serrano

Department of Mechanical Engineering, Lafayette College, Easton, PA, USA

Received: 08 September 2005 / Accepted: 12 May 2006 / Published (online): 01 June 2006

---

### ABSTRACT

This paper discusses the inertia tensors of tennis rackets and their influence on the elbow swing torques in a forehand motion, the loadings transmitted to the elbow from central and eccentric impacts, and the racket acceleration responses from central and eccentric impacts. Inertia tensors of various rackets with similar mass and mass center location were determined by an inertia pendulum and were found to vary considerably in all three orthogonal directions. Tennis swing mechanics and impact analyses were performed using a computer model comprised of a full-body model of a human, a parametric model of the racket, and an impact function. The swing mechanics analysis of a forehand motion determined that inertia values had a moderate linear effect on the pronation-supination elbow torques required to twist the racket, and a minor effect on the flexion-extension and valgus-varus torques. The impact analysis found that mass center inertia values had a considerable effect on the transmitted torques for both longitudinal and latitudinal eccentric impacts and significantly affected all elbow torque components. Racket acceleration responses to central and eccentric impacts were measured experimentally and found to be notably sensitive to impact location and mass center inertia values.

**KEY WORDS:** Biomechanical models, tennis swing, forehand, elbow loads, impact behavior.

---

### INTRODUCTION

An ongoing trend in the tennis equipment industry is designing ever larger racket faces without increased overall racket weight (Coe, 2000). The results are rackets with increased inertia tensor values. Changing the inertia tensor of the tennis racket may have multiple and interconnected effects since the inertia values influence both the tennis player and the behavior of the racket. For example, to some degree a modified inertia tensor may alter the torque necessary to swing the racket, the manner in which

the racket reacts at impact, and the forces and torques transmitted back to the player from impact (Brody, 2000).

While it is understood that changing the racket geometry can affect the inertia values of the racket and resulting tennis swing torques, transmitted torques, and racket behavior, scientific investigations to precisely determine these effects have been limited. Brody (1979) discussed the potential merits of oversized rackets, perimeter weighting, and increased racket head inertia on racket behavior and shot production. Mitchell et al.

(2000) studied the effects of moment of inertia at the racket handle on serving velocity and found an inverse relationship between racket speed and heel inertia. Elliot et al. (1980) found that impact vibrations measured at the racket were reduced for oversized rackets. Kawazoe and Yoshinari (2000) studied the impact shock vibrations at the wrist joint for two oversized rackets and determined that the lighter racket caused higher shock vibrations. Hennig et al. (1992) found that increased racket head size reduced arm vibrations as measured by accelerometers for off-center impacts, however no direct comparisons to racket inertia values were presented. Liu (1983) found that the coefficient of restitution of the ball/racket impact was a function of the ratio of the radius of gyration about the racket pivot to the distance of the geometric center of the racket head to the pivot thus indirectly correlating moment of inertia to COR.

The importance of the elbow joint in swinging the racket is well documented (Bahamonde and Knudson, 2003; Elliott et al., 2003). In addition, the high incidence of overuse injury to this joint is also well known (Priest et al., 1980; Hennig et al., 1992). The forces generated by impact between the racket and the ball, especially off-center impacts have been identified as one of various other factors in the development of tennis elbow (Hennig et al., 1992). Knudson (1991) states that rackets that minimize the effects of off-center impacts should be considered as intervention to reduce the risk of tennis elbow. Thus, it was decided that the most relevant joint to focus on for this study is the elbow, although it was recognized that the wrist and shoulder joints also deserve similar investigations.

The purpose of this study was to investigate the influence of racket inertia properties on the elbow torques during a forehand tennis swing, and the feel of impact at the elbow for central and eccentric impacts, and the acceleration response of the racket to central and eccentric impacts.

## METHODS

### *Inertia properties of tennis rackets*

The inertia properties of a solid body are completely characterized by the 3x3 inertia tensor, which is defined as:

$I_{xx}$	$I_{xy}$	$I_{xz}$
$I_{xy}$	$I_{yy}$	$I_{yz}$
$I_{xz}$	$I_{yz}$	$I_{zz}$

The matrix is symmetric yielding six independent inertia quantities. The terms on the

main diagonal ( $I_{xx}$ ,  $I_{yy}$ , and  $I_{zz}$ ) are the moments of inertia. The off-diagonal terms ( $I_{xy}$ ,  $I_{xz}$ , and  $I_{yz}$ ) are the cross-products of inertia. Together, the elements of the inertia tensor represent the dynamic consequences of the arrangement of the mass of a solid body, a tennis racket in this case, and are a measure of the body's resistance to changes in angular motion. For a body with two planes of symmetry, the products of inertia are zero and the principal axes of inertia orient with the planes of symmetry. For the case of a tennis racket there are two planes of symmetry, the plane of the racket face (Y-Z plane, see Fig. 1), and the plane perpendicular to the face and parallel to the handle (X-Z plane, see Figure 1). Thus the inertia tensor for a tennis racket reduces to the "diagonalized" principal inertia form:

$I_{GX}$	0	0
0	$I_{GY}$	0
0	0	$I_{GZ}$

where  $I_{GX}$ ,  $I_{GY}$ , and  $I_{GZ}$  are the principal moments of inertia of the body, which are computed about the principal axes of inertia located at the racket mass center (CG).

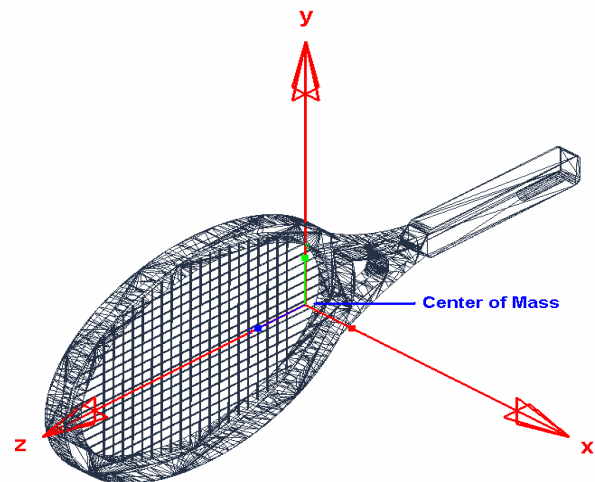


**Figure 1.** Racket mass center principal coordinate system.

A solid body subjected to an unbalanced torque about a principal axis will experience a change in the angular motion about that axis that is inversely proportional to the corresponding principal inertia component. Thus, knowledge of the principal inertias of a solid body is useful in evaluating the dynamic behavior of the body when subjected to unbalanced torques, in this case the swinging torques from a player, and the loadings from impacting the ball.

The values of the inertia tensor elements are functions of both the location and orientation of the coordinate axes to which the tensor is referenced. An

important inertia location on the racket is at the point where the player grips the racket at the handle. Using the Parallel Axis Theorem, the inertia tensor about a parallel axis at the grip point is the following:

$I_{GX} + mL^2$	0	0
0	$I_{GY} + mL^2$	0
0	0	$I_{GZ}$

where  $m$  is the mass of the racket and  $L$  is the distance from the mass center to the grip point.

It is obvious that the racket inertia properties in the X and Y directions increase rapidly as one moves away from the mass center. This fact highlights the importance of the handle length and the mass center location to the inertial “feel” of the racket to the player.

A variety of racket configurations of similar mass and mass center locations were sought in order to obtain realistic racket inertia values in all principal directions; to obtain a sense of the range of possible inertia values in the principal directions; and to determine the relative values of inertia for a given racket. Having a wide range of complete and realistic racket inertia values allows one to better predict the possible range of expected effects of inertia on the tennis swing, the additional loadings from impact, and the racket acceleration response to impacts. Ten rackets were chosen and include a junior racket as well as high quality and oversized rackets.

An inertia pendulum was designed to measure the mass center location and the three principal inertia values of the tennis rackets (Brody, 1985). The pendulum was calibrated with standard shaped objects and included values above and below the expected inertias of the rackets. The calibration objects fit the calibration curve with an  $R^2$  value of 0.999682 (coefficient of determination). The device

was accurate to 1.5% and repeatable to 0.5%

The mass and inertia properties of the rackets are given in Table 1. Mass center locations are measured from the end of the handle. In addition, the parallel axis theorem was used to determine the racket inertia values about a parallel coordinate system placed 75mm from the end of the handle. These values are given in Table 2. Table 2 also lists the quantity  $ML^2$  which represents the additional inertia contribution in both the X and Y directions by moving the mass center inertia to the handle grip point. The Z direction inertia is unchanged at the handle relative to the mass center.

Referring to Table 1,  $I_{GX}$  is consistently the largest mass center inertia value for all the rackets,  $I_{GY}$  is slightly smaller than  $I_{GX}$  in all cases, and  $I_{GZ}$  is by far the smallest inertia value. The contribution of the handle length to the  $I_{GX}$  and  $I_{GY}$  values is considerable and accounts for the large difference between  $I_{GX}$  and  $I_{GY}$ , and  $I_{GZ}$ . Table 1 also reveals that while the racket masses and mass center locations are not too different among the rackets, the inertia values in all three directions vary considerably. The greatest relative difference among the rackets occurred about the Z-axis. Thus it appears from this sample that racket designers can successfully manipulate racket inertia values for a narrow range of mass and CG locations. Table 2 reveals that the inertias of the racket at the handle grip point are considerably larger about the X and Y axes than at the mass center. The additional inertia contribution at the handle is the  $ML^2$  term which accounts for approximately 45 to 60% of the  $I_{HX}$  and  $I_{HY}$  inertia values at the handle. Brody (1985) refers to  $I_{HY}$  inertia as the “swing weight,” because it is a measure of how “heavy” the racket feels when you swing it and what the racket’s “hitting mass” is when the ball is struck, and the  $I_{HX}$  inertia as an important resisting quantity when executing “slice” or “chop” shots or when serving.

**Table 1.** Racket Mass, Mass Center Location, and Principal Inertia Values

Racket	Mass (kg)	CG Loc (mm)	$I_{GX}$ ( $\text{kg}\cdot\text{mm}^{-1}\cdot\text{s}^{-2}$ )	$I_{GY}$ ( $\text{kg}\cdot\text{mm}^{-1}\cdot\text{s}^{-2}$ )	$I_{GZ}$ ( $\text{kg}\cdot\text{mm}^{-1}\cdot\text{s}^{-2}$ )
1	.314	346.6	16104.9	14407.0	987.1
2	.309	360.6	18270.5	16336.6	885.7
3	.345	330.4	16624.8	15048.6	1266.7
4	.318	331.3	16175.4	14445.1	1319.0
5	.332	326.6	15704.8	14019.0	1186.4
6	.324	314.6	14612.8	13394.1	1007.3
7	.315	320.0	12348.9	11227.3	1029.4
8	.301	305.4	11007.2	9904.7	889.2
9	.273	283.2	9224.8	7982.8	739.9
10	.253	272.0	8118.7	7126.6	448.8
<b>Average</b>	<b>.308</b>	<b>319.1</b>	<b>13819.3</b>	<b>12389.2</b>	<b>975.9</b>

**Table 2.** Racket inertia values about the handle grip point.

Racket	$I_{HX}$ ( $\text{kg}\cdot\text{mm}\cdot\text{s}^{-2}$ )	$I_{HY}$ ( $\text{kg}\cdot\text{mm}^{-1}\cdot\text{s}^{-2}$ )	$I_{HZ}$ ( $\text{kg}\cdot\text{mm}^{-1}\cdot\text{s}^{-2}$ )	$ML^2$ ( $\text{kg}\cdot\text{mm}^{-1}\cdot\text{s}^{-2}$ )
1	39138.4	37440.4	987.1	23033
2	43368.7	41434.7	885.7	25098
3	39064.5	37488.3	1266.7	22439
4	36986.9	35256.6	1319.0	20811
5	36622.5	34936.8	1186.4	20917
6	33026.8	31808.1	1007.3	18414
7	29557.9	28436.3	1029.4	17209
8	26678.2	25575.7	889.2	15671
9	16905.2	15663.2	739.9	7680
10	19546.0	18553.9	448.8	11427
<b>Average</b>	<b>32089.5</b>	<b>30659.4</b>	<b>975.9</b>	<b>18269.9</b>

### Computer model

A full-body model of a human coupled to a parametric model of a tennis racket was developed to determine racket and arm trajectories, player/racket interaction forces and torques, joint motions, forces, and torques, and reactions to impact (see Figure 2). The model included a spring-damper impact function to simulate ball-racket impact and a ground surface model to support the model through contact with the feet. This modeling approach has been used to analyze the golf swing (Nesbit et al., 1994; Nesbit, 2003a; 2003b), golf equipment behavior (Nesbit et al., 1996), and other sport biomechanical motions (Nesbit and Ribadeneira, 2003).

**Figure 2.** Computer model of forehand tennis swing.

The model was built, analyzed, and post-processed with the aid of the commercial software packages ADAMS (Mechanical Dynamics, Inc.) and LifeMod humanoid pre-processor (Biomechanics Research Group, Inc.). ADAMS is a multi-body dynamic analysis program where models are built from rigid segments connected with flexible elements and/or a variety of joints. Forces and motions can be superimposed upon the model. ADAMS derives the differential equations of motion for the model employing methods of Lagrangian dynamics. The equations of motion are solved using

one of several backward differentiation formula (BDF) integrators. The results are output and the model is simulated using the ADAMS postprocessor.

### Humanoid model

The LifeMod program is a pre-processor of the ADAMS software designed to aide in the creation of humanoid models from ADAMS modeling elements. LifeMod was used to model the player as a variable full-body, multi-link, three-dimensional humanoid mechanism made up of seventeen rigid segments interconnected with joints. The model was configured with the following fifteen body segments; head, neck, thorax, lumbar, pelvic, upper arm (2), forearm (2), thigh (2), lower leg (2), hand (2), and foot (2). All segments were geometrically defined by their adjacent joints with exceptions of the neck (C1-C8), thorax (T1-T12), and lumbar (L1-L5 and S1-S5) which were defined by the associated vertebrae. The segment size, mass and inertia properties were determined from gender, age, and overall body height and weight using the GeBod data base accessible through the ADAMS software. The model consisted of the following sixteen joints; ankles (2), knees (2), hips (2), lumbar, thoracic, neck, shoulders (2), elbows (2), and wrists (2). All joints were spherical yielding a maximum of three relative angular degrees-of-freedom with the exceptions of the knees, elbows, and wrists which were modeled as two degree-of-freedom joints (bending and twisting for the knees and elbows, bending and yawing for the wrists). The motions superimposed upon the joints were specified in terms of Bryant angles (see below) and their time dependent derivatives.

The body segment reference coordinate systems, established when the model is posed in the standard anatomical position, places the Z-axis pointing downward with the exception of the feet which point forward parallel to the long axis of the

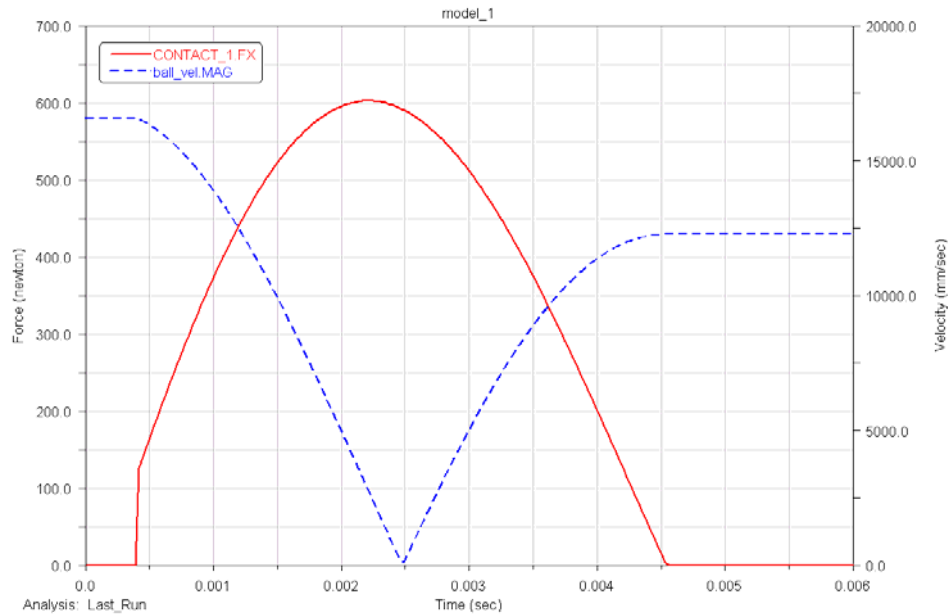


**Figure 3.** Impact model forces and racket/ball relative velocity.

foot segment. The X-axis points outward from the body, and the Y-axis completes a right-handed coordinate system. Joint motions, forces, and torques are of the distal body segment coordinate system relative to the proximal body segment coordinate system. The angular quantities are specified according to the relative body (Euler angle) 1-2-3 Bryant angle convention where alpha motion ( $\alpha$ ) is about the X-axis, beta motion ( $\beta$ ) is about the Y'-axis, and gamma motion ( $\gamma$ ) is about the Z''-axis (Kane et al., 1983). The elbow joint is capable of flexion-extension (beta motion) and pronation-supination (gamma motion). The varus-valgus reaction torque in the plane formed by upper arm and forearm is in the alpha direction. Note that positive elbow torques indicate flexion, valgus, and pronation.

#### **Ground surface model**

A ground surface model was added to support the humanoid model. A standard linear spring-damper system was used to represent the contact between the feet and the ground, and frictional forces provided traction. The initial contact parameters were obtained from Scott et al. (1993) and were adjusted at solution time to prevent over-stiffening the model. The humanoid model was balanced by kinematically driving the angular DOF's of the lower torso segment (hips) relative to the global coordinate system. To avoid over-constraining the model, the linear DOF's were set free. A kinematically driven model is infinitely stiff, therefore small joint angle errors can cause one of the feet to lose contact with the ground surface. To solve this problem, the Beta motion (flexion-extension) of one of the ankle joints was

dynamically driven with a torque control function (Nesbit et al., 1994) to give the model compliance.

#### **Racket and impact models**

The tennis racket was modeled as a rigid structure with representative mass and inertia properties. The connection between the racket and the hand was modeled as perfectly rigid with no damping. This rigid body approach to the modeling of the human and racket was similar to the methods of Bahamonde and Knudson (2003) and Elliot et al. (2003) in studying swing mechanics. The rigid connection will yield the maximum transmitted forces and torques from the racket/ball impact. While the tennis literature recognizes the influence and effects of grip tightness and arm damping on transmitted vibrations (Hennig et al., 1992), no definitive conclusions have emerged on how to properly interconnect human and racket models at this time. Thus the predicted relative effects of inertia on transmitted forces and torques at the elbow should be given more weight than the absolute effects as determined from these computer models.

The impact model (Eqn. (1)) combines the spring rates and damping of the racket strings and tennis ball, and is a function of their relative deflection ( $X$ ) and speed ( $V_{rel}$ ). From the work of Cross (2000), the combined spring rate of the ball and racket strings ( $K$ ) was estimated to be  $30 \text{ kN}\cdot\text{m}^{-1}$ . From the work of Dignall and Haake (2000), the exponent on the deflection was specified as 2 and the effective combined damping ( $C$ ) as approximately  $7.5 \text{ Ns}\cdot\text{m}^{-1}$ . The resulting impact force and racket/ball relative velocity are shown in Figure 3. For this case, the function yielded a maximum impact force of 600 N, a coefficient of

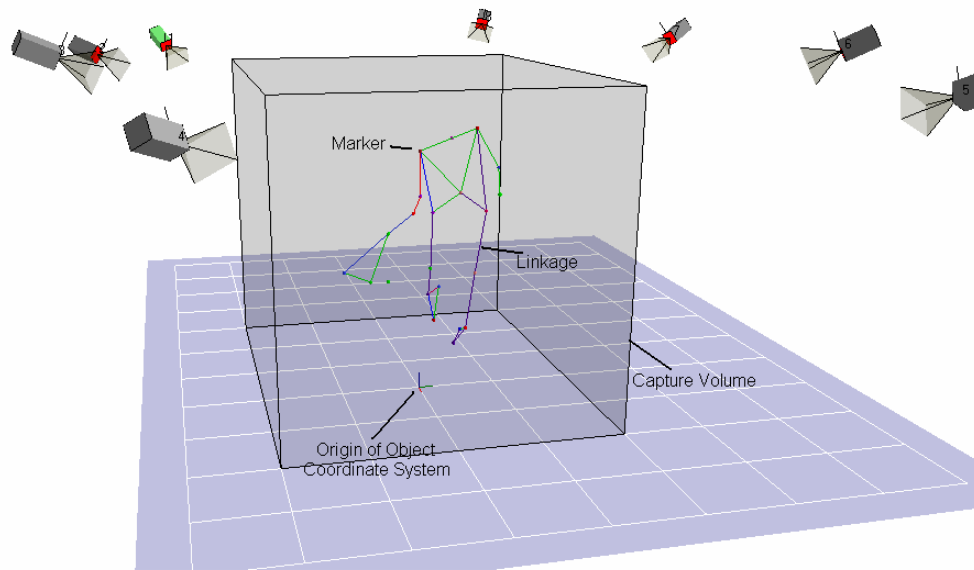


**Figure 4.** Working volume and stick figure model of recorded tennis swing.

restitution of 0.74, and an impact duration of 0.0041 seconds. These values agree with Carre et al. (2003) whose analytical methods predict a spring rate of  $32.3 \text{ kN}\cdot\text{m}^{-1}$  and damping of  $8.1 \text{ N}\cdot\text{s}\cdot\text{m}^{-1}$  for the impact duration and coefficient of restitution found for this impact model.

$$\text{Force} = K * X^{\text{exp}} + C * V_{\text{rel}} \quad (1)$$

#### **Swing data and joint motions**

Data to kinematically drive the joints of the player model were obtained from subject forehand swings. A multi-camera motion analysis system tracked passive-reflective markers (13 and 19 mm in diameter) that were strategically placed upon the player and the racket. There were 23 markers placed on the player, and three on the racket. On the player the markers were located at the wrists, forearms, elbows, shoulders, cervical and lumbar vertebra, head, hips, knees, mid lower leg, ankles, and feet. All markers were located relative to bony landmarks for consistency, and securely attached with two-sided tape (skin) or Velcro (clothing). Markers were attached directly to the skin wherever possible. Subjects wore snug-fitting clothing (tank-top and bicycle-style shorts), a baseball hat (head marker), and shoes of their choice. Marker/joint offsets were measured, and virtual joint-center markers were located from these data using features provided by the data collection software. Reflective tape was attached to the tennis ball to determine the precise time of impact. Figure 4 shows the camera locations, the working volume, global origin, and a stick figure representation of the subject swing.

The three-dimensional marker paths were recorded at 200Hz then smoothed and processed to

yield global body 1-2-3 angular motions of each body segment and the racket. The global angular motions were transformed into local relative joint motions (position angles) by comparing the motions of adjacent body segments using processes described in Craig (1986). These relative angular motions were used to kinematically drive the joints of the player model.

#### **Solution of model**

The primary components of the model, the humanoid and racket, are rigid and kinematically driven via local relative joint position angles yielding simultaneous linear equations which results in a closed-form solution. However the ground-surface and the impact force models introduced non-linearities and time-dependent dynamic responses into the system. Thus, the entirety of the model represents a forward dynamics or simulation problem requiring numerical integration to solve. The resulting dynamic equations of motion were solved using a Wielenga Stiff Integrator (Mechanical Dynamics Inc.). Solution of the model yielded a simulation of the swing, player/racket interaction forces and torques, joint angular velocities and accelerations, joint torques and reaction forces, impact forces, and transmitted impact loads.

#### **Subject**

One female subject was used to obtain the swing data for this study. The subject was a member of the Lafayette College tennis team. The subject was right-handed, 22 years old, 1.65m tall, and 56.7 kg in weight. She had been playing for 15 years, with ten of those under the guidance of a coach. The

**Table 3.** Maximum elbow swing torque components before impact.

Racket	Max Elbow Torques (Nm)		
	Valgus-Varus	Pronation-Supination	Flexion-Extension
1	30.66	3.78	14.07
2	31.60	3.48	14.36
3	30.75	5.75	14.15
4	29.59	6.07	13.91
5	29.75	4.83	13.68
6	28.70	4.19	13.76
7	28.53	4.42	13.65
8	27.87	3.56	13.29
9	26.33	2.91	12.59
10	27.11	1.72	13.22

subject was free to select any racket from the ten in this study without knowing their mass and inertia properties. The subject had reflective markers placed upon her body and the racket. After practicing for several minutes to acclimate to the markers, racket, and surroundings, the subject was asked to execute a series of closed-stance forehand swings which included striking a ball. A swing from the subject was self-selected based upon her assessment of the stick figure animations, then analysed using the computer models described above.

## RESULTS AND DISCUSSION

Using the same swing from the subject, the racket inertia properties for each of the ten rackets were input into the racket model and the entire model reanalyzed. The racket mass and mass center locations were normalized within the racket model to reflect the average values of the rackets (see Table 1). Using the same mass and CG location for all the rackets removed these variables from the analyses, thus any difference in swing torque values for the

rackets was a direct result of their differing inertia properties. Table 3 presents the maximum values of the elbow swing torque components for the subject during the time period between the initiation of the forward swing to just before impact. These values agree well with Bahamonde and Knudson (2003) who report elbow torque profiles for both open and square stance forehand tennis swings.

The elbow torque components were correlated to the three mass center inertia values, the three inertia values at the handle grip point, and  $ML^2$ , the difference in inertia between the two locations. The strongest relationships are shown in Figures 5 and 6.

Figure 5 illustrates a strong linear relationship between the pronation-supination torque in the forearm and the value of  $I_{GZ}$ . This finding is predicted by Newton's 2<sup>nd</sup> Law for rotational systems. At the time of peak pronation-supination torque, the long axis of the forearm is closely coincident with the long axis of the racket. In this position the primary retarding quantity of the racket is  $I_{GZ}$ . For the flexion-extension and valgus-varus torques, the strongest relationships are with the  $ML^2$

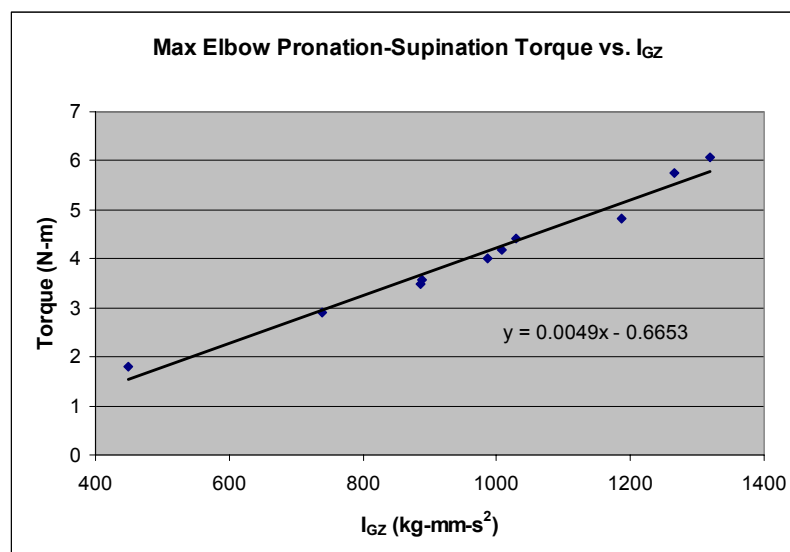


**Figure 5.** Maximum elbow pronation-supination torque vs. racket  $I_{GZ}$

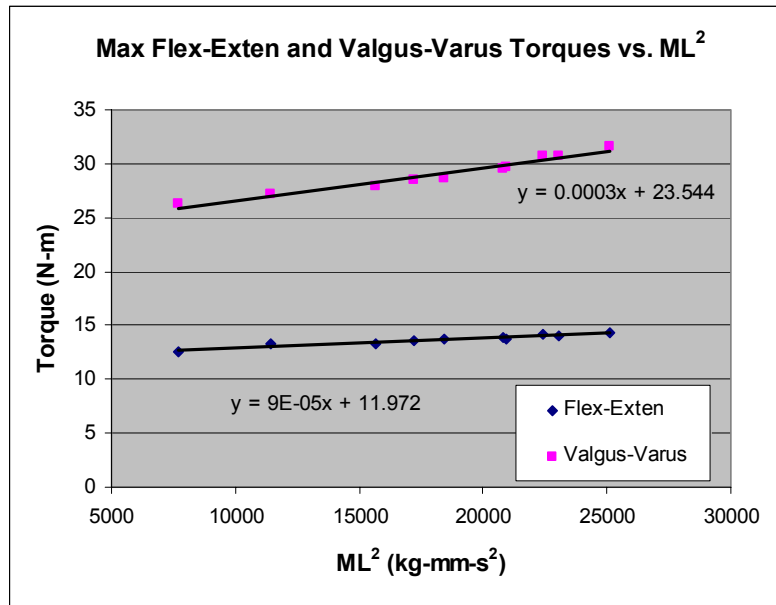


Figure 6. Maximum flexion-extension and valgus-varus torques vs.  $ML^2$

contribution to the inertia at the racket handle grip point in the X and Y directions (Figure 6). However, the actual effects of  $ML^2$  on the two torque components are fairly insignificant as noted by the shallow slopes, small ranges of torque values, and high values of the y-intercepts. The relationships among the flexion-extension and valgus-varus torques with the X and Y inertia values at the racket handle are nearly as strong as with the  $ML^2$  inertia, yet these actual effects are insignificant as well for the same reasons. The torques generated and reacted in the flexion-extension and valgus-varus directions are far more effected by the overall mass and mass center location of the racket than its inertia at the handle or mass center.

A limitation of this study is the assumption that the subject will swing at the same speed regardless of the racket inertia values. This assumption was necessary to isolate the various effects of racket inertia on the elbow from the effects of racket head speed. An analysis of the elbow torques in Table 3 indicates that it is a reasonable assumption for the flexion-extension and valgus-varus directions. However, the considerable range of the pronation-supination torques implies that the twisting velocity of the racket may be affected by the inertia values in this direction. Using these pronation-supination torque values to redrive the model kinetically would verify that the twisting velocities would be a function of racket inertia.

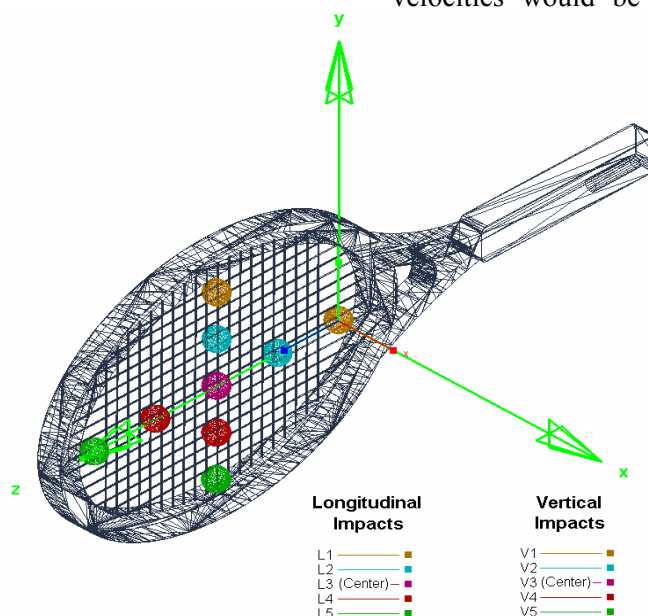
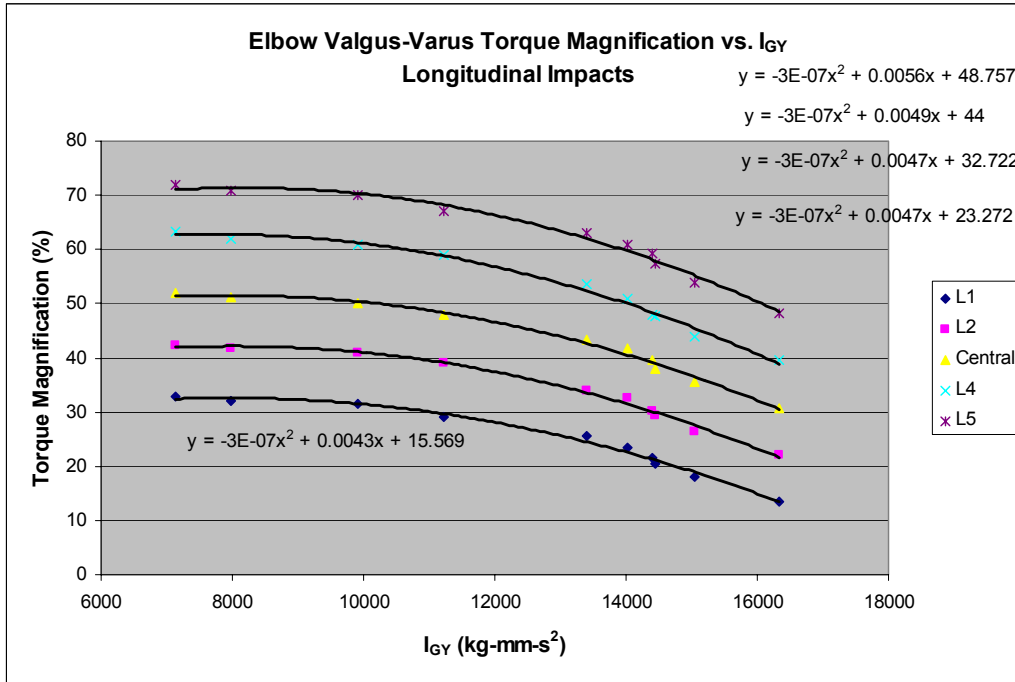


Figure 7. Central and eccentric impact positions.





**Figure 8.** Valgus-varus torque magnification vs.  $I_{GY}$  for longitudinally displaced impacts.

However, this type of analysis ignores the feedback effects of the subject in attempting to maintain a kinematically consistent swing regardless of racket inertia properties. The computer modeling approach cannot presently resolve this issue, thus the results presented in this paper must be tempered by this limitation of the model.

**Impact analysis: Computer results**

Several investigators have shown that eccentric impacts increase the impact reaction loading to the player (Elliot, 1982; Henning, et al., 1992; Kawazoe

and Yoshinari, 2000; Knudson, 1991). Inferences to the effects of racket inertia via increased head size on reducing this transmitted impact force have been made by Henning, et al. (1992) and Knudson (1991; 2004), yet no study has quantified the relationships of racket inertia properties on the transmitted loadings. Thus the computer model with the impact force function added was used to study the effects of racket inertia properties on the transmitted forces from impact on the elbow. Central impact as well as laterally and vertically displaced eccentric impacts were investigated (Figure 7). For this study, central

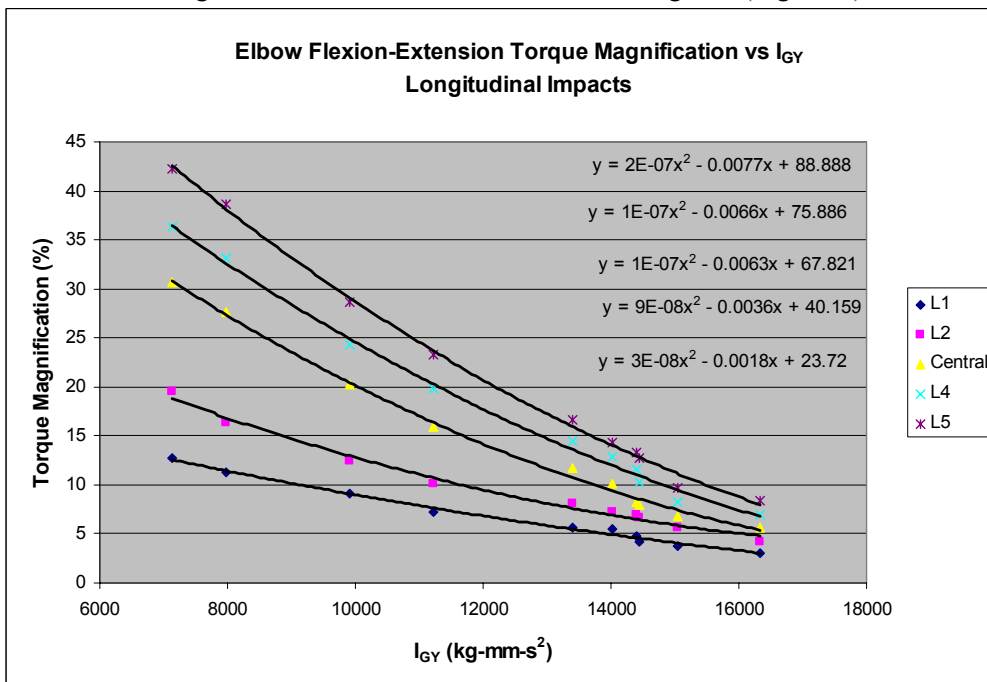


**Figure 9.** Flexion-extension torque magnification vs.  $I_{GY}$  for longitudinally displaced impacts.

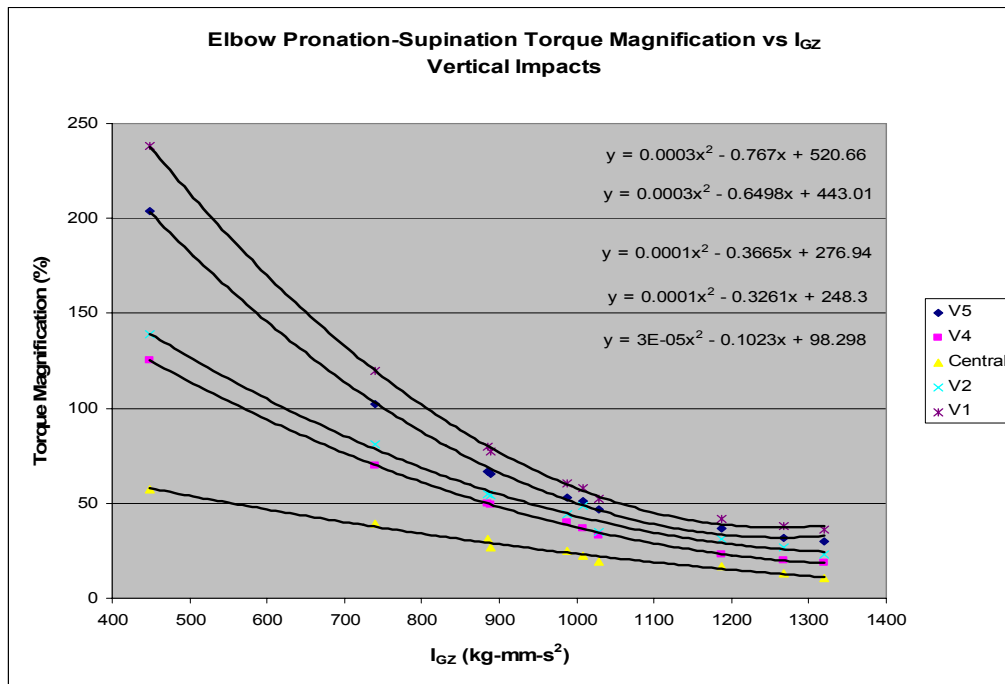


**Figure 10.** Pronation-supination torque magnification vs.  $I_{GZ}$  for vertically displaced impacts.

impact is defined as impact at the geometric center of the racket face. The nine impact locations shown in Figure 7 were applied to each of the ten rackets subjected to the same subject swing. The racket mass and mass center locations were normalized to the average values as before. In addition, the distance from the grip point to the geometric center of the racket face was normalized for all the rackets.

The peak elbow torques in each of the component directions occurring just after impact were recorded for the various impact locations. These elbow torque components resulting from the transmitted impact loadings ( $T_{impact}$ ) were compared to the maximum pre-impact swing torque components ( $T_{swing}$ ), and an impact magnification factor calculated with the following equation:

$$MF = \frac{T_{impact} - T_{swing}}{T_{swing}} * 100 \quad (2)$$

The elbow torque magnification factors were then correlated to the racket inertia properties at the mass center and the handle grip point. The strongest relationships are shown in Figures 8 through 10. These figures illustrate the relationships among specific racket inertia properties and related component torque magnification factors for particular directions of eccentric impacts. Each line in the figures represents a specific impact location on the racket face. Also included on each figure are 2<sup>nd</sup> order polynomial curve fits associated with each impact location listed in the same vertical order as the data curves. There is general agreement with

Kawazoe and Yoshinari (2000) regarding the trends of the transmitted impulse magnitudes at the elbow and the location of the impact, as well as the diminishing effects of increased racket size on transmitted impulses (for two rackets only however).

Figure 8 illustrates the valgus-varus torque magnification factor versus the mass center inertia in the Y-direction for longitudinally displaced impacts. Longitudinally displaced impacts have the potential to cause the largest absolute increase in elbow torque (45 N-m maximum for the valgus-varus torque component). This effect can be diminished by increasing the  $I_{GY}$  value of the racket. As shown by the figure, there is a 2<sup>nd</sup> order inverse relationship between  $I_{GY}$  and the transmitted valgus-varus torque at the elbow for longitudinally displaced eccentric impacts. Impacts outside the geometric center of the racket face have a greater effect on the transmitted torques than inside the face center. This result may be due to the shortening of the moment arm from the impact location to the racket mass center as well as moving nearer to the center of percussion (Elliot, 1982).

Figure 9 illustrates the flexion-extension torque magnification factor versus the mass center inertia in the Y-direction for longitudinally displaced impacts. Longitudinally displaced impacts also have the potential to cause large increases in elbow flexion-extension torque. This effect is smaller both in absolute value (18.9 Nm maximum) and relative value (43% maximum) than for valgus-varus torques. Similarly, this effect can be diminished by increasing the  $I_{GY}$  value of the racket. As shown by the figure, there is a nearly inverse linear

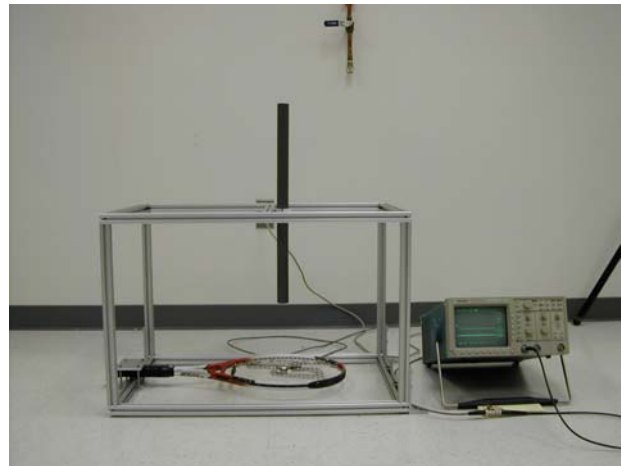
relationship between  $I_{GY}$  and the transmitted flexion-extension torque at the elbow for longitudinally displaced eccentric impacts. Impacts outside the geometric center of the racket face also have a greater effect on the transmitted torques than inside the face center for the same reasons as described above.

Figure 10 illustrates the pronation-supination torque magnification factor versus the mass center inertia in the Z-direction for vertically displaced impacts. Vertically displaced impacts can cause the largest relative increase in elbow torque (238% maximum for the pronation-supination torque component). This is also the type of eccentric impact where racket inertia properties have the greatest effect in diminishing the transmitted torque magnification potential. This finding agrees with discussions by Brody (1985). As shown by the figure, there is a strong 2<sup>nd</sup> order inverse relationship between  $I_{GZ}$  and the transmitted pronation-supination torque at the elbow for vertically displaced eccentric impacts. Impacts above the geometric center of the racket face have a slightly greater effect on the transmitted torques than below the face center a finding supported by Knudson (1991). This result is due to the sign on the swing pronation-supination torque component which is opposite for impacts above the face center, and the same for impacts below the face center. When interpreting Figure 10, one must keep in mind the relatively small values of swing pronation-supination torque (Table 3), and the strong linear relationship between the swing pronation-supination torque and  $I_{GZ}$  (Figure 5).

The results of the computer analyses predict that racket inertia properties appreciably affect the transmitted impact torques at the elbow. The rigid nature of the computer model and the invariantly driven kinematic nature of the joints serve to overestimate the importance of racket inertia in diminishing the transmitted torques. The model lacks soft tissue elasticity and damping that would serve to absorb and dissipate a portion of the impact energy. Thus the energy of impact is absorbed (conservatively) and released by the mass and inertia elements of the model instead of being distributed among the elastic and dissipative elements as well. The trends predicted by the model are generally supported by Newton's Laws for a rigid system. The polynomial relationships in the figures seem to suggest some sort of coupling effect among the mass and inertia properties, elbow kinematics, and/or racket trajectory since Newton's Laws would have predicted more linear relationships for one degree-of-freedom motion. This observation is supported in the experimental studies discussed below.

### **Impact analysis: Experimental results**

The impact responses of each racket to central and eccentric impacts were evaluated experimentally (see Figure 11). The rackets were clamped in a cantilever manner at the handle grip point and impacted by a 67.15 gram steel ball dropped from a height of 762 mm at the various locations indicated by Figure 7. The distance from the center of the racket faces to the cantilever clamping point was normalized for all rackets. However the interpretations of the results must be tempered by the small but important differences in string tension, frame stiffness, mass, and CG location of the rackets. A uni-axial accelerometer (Omega Acc 787A-0107) was mounted to the frame of the racket at the top for longitudinally displaced impacts, and at the side for vertically displaced impacts. The accelerometer output was recorded and displayed by a Tektronix TDS 320 oscilloscope.



**Figure 11.** Impact testing apparatus.

Each impact location for each racket was tested five times then averaged. The test repeatability was within 10% for all cases. The peak acceleration values were linearly correlated to  $I_{GY}$  for longitudinally displaced impacts (Figure 12) and  $I_{GZ}$  for vertically displaced impacts (Figure 13). Each line in the figures represents a specific impact location on the racket face. It was only necessary to test one side of the racket face for vertically displaced impacts because of symmetry. Also included on each figure is the  $R^2$  value for each impact location listed in the same vertical order as the data curves.

Figure 12 illustrates the linear relationship between impact induced accelerations measured at the top edge of the racket frame versus  $I_{GY}$  for longitudinally displaced impacts. The magnitude of the accelerations are strongly dependent upon impact location and increase as the impact point moves laterally away from the mass center. As

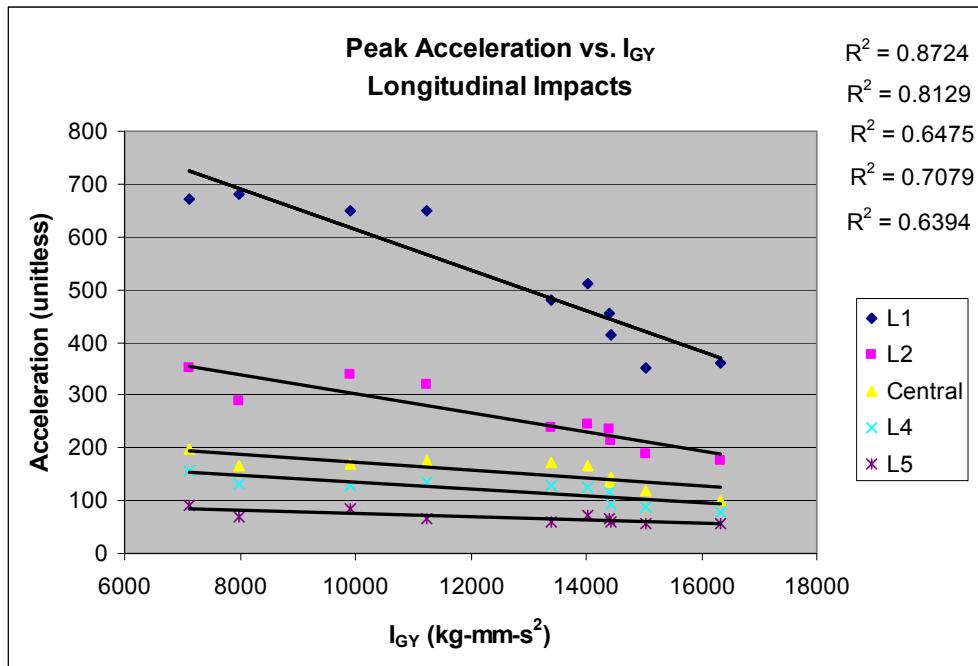


**Figure 12.** Measured peak acceleration vs.  $I_{GY}$  for longitudinally displaced impacts.

expected however, this effect is inversely related to the  $I_{GY}$  value of the racket which serves to reduce the accelerations by nearly a factor of two between the extreme values of  $I_{GY}$  for all impact locations.

Figure 13 shows the linear relationship between impact induced accelerations measured at the side edge of the racket frame versus  $I_{GZ}$  for vertically displaced impacts. The magnitude of the accelerations are also strongly dependent upon impact location and increase rapidly as the impact point moves vertically away from the mass center. Again, this effect is inversely related to the  $I_{GZ}$  value

of the racket. It appears from the data that  $I_{GZ}$  effects the accelerations by nearly a factor of four between the extreme values of  $I_{GZ}$  for all impact locations. However, there is a coupling of racket twisting and bending responses at this accelerometer location which may cause the  $I_{GY}$  value of the rackets to effect these results thus exaggerating the effects of  $I_{GZ}$ .

It is clear from the results of these experiments that racket inertia properties affect the impact vibratory response of the rackets. These findings are supported by Elliot et al. (1980). However, the net

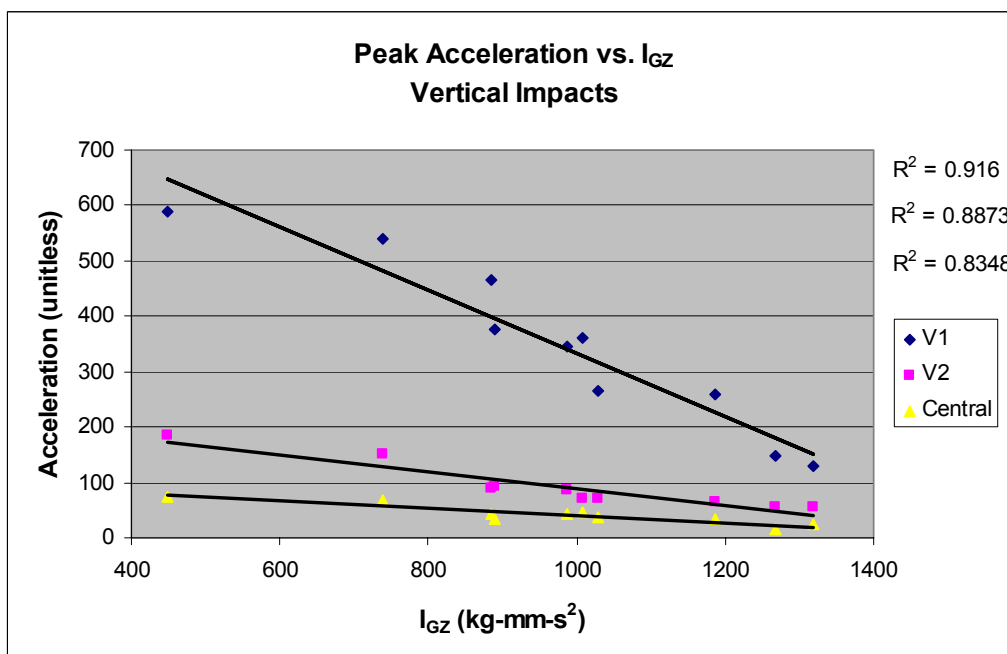


**Figure 13.** Measured peak acceleration vs.  $I_{GZ}$  for vertically displaced impacts.

effects of these experimental findings on the elbow are uncertain. As stated by Knudson (2004), the small size of impact induced frame vibration forces, their limited energy, and their quick damping by hand forces suggests that vibration is not a major cause of tennis elbow. The works of Hennig et al. (1992), Kawazoe and Yoshinari (2000), and Elliot (1982) taken together demonstrate that impact induced vibrations at the racket are diminished substantially as they propagate from the racket frame through the hand, wrist, and forearm before reaching the elbow. It is also not clear from the literature how these impact vibrations are related to the transmitted impact loadings, sometimes referred to as impulse loadings, determined by the computer model. Knudson (2004) separates the effects of the impact vibratory response and the impact impulse response relative to elbow impact loadings and states that it is the large impulse forces that creates the recoil of the racket which rapidly stretches the muscles of the forearm and that off-center impacts increase impulse forces. A further refined computer model containing a flexible racket frame, variable grip pressure, and anatomical damping may serve to clarify these issues.

## CONCLUSION

Racket mass property measurements using an inertia pendulum found that inertia tensors of various rackets with similar mass and mass center location can vary considerably in all three orthogonal directions. Quantifying how these wide ranging inertia values affect the elbow swing torques, and the impact induced transmitted torques at the elbow for a forehand motion were the objectives of this work. Tennis swing mechanics and impact analyses were performed using a computer model comprised of a full-body model of a human, a parametric model of the racket, and an impact function. The stiffness of the model coupled with the invariant kinematically driven motion of the model joints may have overestimated the absolute results predicted by the model, however there is confidence that the trends found are reasonable. The swing mechanics analysis at the elbow determined that the inertia values about the long axis of the racket significantly influenced the pronation-supination torque. Little other effect on elbow swing torque from racket inertia were found. The impact analyses found that mass center inertia values had a considerable effect on the transmitted torques for both longitudinal and latitudinal eccentric impacts and significantly affected all elbow torque components. Racket acceleration responses to central and eccentric impacts were measured experimentally and found to

be notably sensitive to impact location and mass center inertia values. However, the net effects of these experimental findings on the elbow are uncertain because of anatomical damping and grip pressure effects which serve to greatly diminish these vibrations at the elbow.

## ACKNOWLEDGEMENTS

Funding for this project was provided by a grant from the National Science Foundation.

## REFERENCES

- Bahamonde, R.E. and Knudson, D. (2003) Kinetics of the upper extremity in the open and square stance tennis forehand. *Journal of Science and Medicine in Sport* **6**, 88-101.
- Brody, H. (1979) Physics of the tennis racket. *American Journal of Physics* **47**(6), 482-487.
- Brody, H. (1985) The moment of inertia of the tennis racket. *The Physics Teacher* **23**, 213-216.
- Brody, H. (2000) An overview of racket technology. In: *Tennis Science and Technology*. Eds: Haake, S.J. and Coe, A. Blackwell Science Ltd, London, England. 43-48.
- Carre, M.J., Goodwill, S.R. and Haake, S.J. (2003) The dynamic characteristics of tennis balls with tennis rackets. *Journal of Sports Sciences* **21**, 839-851.
- Coe, A. (2000) The balance between technology and tradition in tennis. In: *Tennis Science and Technology*. Eds: Haake, S.J. and Coe, A. Blackwell Science Ltd, London, England. 3-40.
- Craig, J.J. (1986) Introduction to robotics: mechanics & control. Reading, Massachusetts: Addison-Wesley Publishing Co.
- Cross, R. (2000) Dynamic testing of tennis balls. In: *Tennis Science and Technology*. Eds: Haake, S.J. and Coe, A. Blackwell Science Ltd, London, England. 175-182.
- Dignall, R.J. and Haake, S.J. (2000) Analytical modeling of the impact of tennis balls on court surfaces. In: *Tennis Science and Technology*. Eds: Haake, S.J. and Coe, A. Blackwell Science Ltd, London, England. 155-162.
- Elliot, B., Blanksby, B. and Ellis, R. (1980) Vibration and rebound velocity characteristics of conventional and oversized tennis rackets. *Research Quarterly for Exercise and Sport* **51**, 608-615.
- Elliot, B. (1982) Tennis: the influence of grip tightness on reaction impulse and rebound velocity. *Medicine and Science in Sports and Exercise* **14**, 348-352.
- Elliott, B., Fleisig, G., Nicholls and Escamilla, R. (2003) Technique effects on upper limb loading in the tennis serve. *Journal of Science and Medicine in Sport* **6**, 76-87.
- Hennig, E.M., Rosenbaum, D. and Milani, T.L. (1992) Transfer of tennis racket vibrations onto the human forearm. *Medicine and Science in Sports and Exercise* **24**, 1134-1140.

- Kane, T.R., Likins, P.W. and Levinson, D.A. (1983) *Spacecraft dynamics*. New York: McGraw-Hill Co.
- Kawazoe, Y. and Yoshinari, K. (2000) Prediction of the impact shock vibrations of the player's wrist joint: comparison between two super large sized rackets with different frame mass distribution. In: *Tennis Science and Technology*. Eds: Haake, S.J. and Coe, A. Blackwell Science Ltd, London, England. 91-99.
- Knudson, D. (1991) Factors affecting force loading on the hand in the tennis forehand. *The Journal of Sports Medicine and Physical Fitness* **31**, 527-531.
- Knudson, D. (2004) What happens at impact and why it can hurt. Coaches Information Service Website. Available from URL: <http://www.coachesinfo.com>.
- Liu, K.Y. (1983) Mechanical analysis of racket and ball during impact. *Medicine and Science in Sports and Exercise* **15**, 388-392.
- Mitchell, S.R., Jones, R. and Kotze, J. (2000) The influence of racket moment of inertia during the tennis serve: 3-dimensional analysis. In: *Tennis Science and Technology*. Eds: Haake, S.J. and Coe, A. Blackwell Science Ltd, London, England. 57-65.
- Nesbit, S.M., Cole, J.S., Hartzell, T.A., Oglesby, K.A. and Radich, A.F. (1994) Dynamic model and computer simulation of a golf swing. *Proceedings of the 1994 World Scientific Congress of Golf, St. Andrews, Scotland*. Eds: Cochran, A.J. and Farrally, M.R. 71-76.
- Nesbit, S.M., Hartzell, T.A., Nalevanko, J.C., Starr, R. M., White, M.G., Anderson, J.R., and Gerlacki, J.N. (1996) A discussion of iron golf club head inertia tensors and their effects on the golfer. *Journal of Applied Biomechanics* **12**, 449-469.
- Nesbit, S.M. (2003a) 3-D mechanics of the wrist during the golf swing. *Proceedings of the American College of Sports Medicine Annual Conference, San Francisco, CA*. Book of abstract. 307.
- Nesbit, S.M. (2003b) Work and power analysis of the golf swing. *Proceedings of the 2003 ASME Annual Bioengineering Conference, Miami, FL*. Book of abstract. 199.
- Nesbit, S.M. and Ribadeneira, M.X. (2003) Sport biomechanical analysis using full-body computer models. *Proceedings of the 2003 IASTED International Conference on Modeling and Simulation, Palm Springs, CA*. Book of abstract. 252-257.
- Priest, J.D., Braden, V. and Gerberish, S.G. (1980) The elbow and tennis, part 1: an analysis of players with and without pain. *Physician and Sports Medicine* **8**, 80-91.
- Scott, S. and Winter, D., (1993) Biomechanical model of the human foot: kinematics and kinetics during the stance phase of walking. *Journal of Biomechanics* **26**, 1091-1104.

## AUTHORS BIOGRAPHY



### Steven NESBIT

#### Employment

Associate Professor and Head, Department of Mechanical Engineering, Lafayette College, Easton, PA, USA.

#### Degree

PhD, PE, MS, BS

#### Research interests

Sports biomechanics, mechanisms, computer modelling.

**E-mail:** [nesbits@lafayette.edu](mailto:nesbits@lafayette.edu)

### Michael ELZINGA

#### Employment

Mechanical engineering student

#### Degree

BS '07

#### Research interests

Bioengineering

**E-mail:** [elzingam@lafayette.edu](mailto:elzingam@lafayette.edu)

### Catherine HERCHENRODER

#### Employment

Mechanical engineer

#### Degree

BS

#### Research interests

Mechanical design

**E-mail:** [herchenc@lafayette.edu](mailto:herchenc@lafayette.edu)



### Monika SERRANO

#### Employment

Mechanical engineer.

#### Degree

BS

#### Research interests

Sports biomechanics.

**E-mail:** [sesam182@hotmail.com](mailto:sesam182@hotmail.com)

## KEY POINTS

- Tennis biomechanics.
- Racket inertia tensor.
- Impact analysis.
- Full-body computer model.

### ✉ Steven M. Nesbit, PhD, PE

Department of Mechanical Engineering, Lafayette College, Easton, PA, USA.